Supporting Information

Inorganic Salt Transition States: A Stable and Highly Stretchable Elastomer Like Phase (ELP) of Phosphate Salts at the Air-Solid Interface

Ya Wang,[a] Rongzhan Fu,[a] Zhiguang Duan,[a] Xijuan Jiang, Chenhui Zhu, and Daidi Fan *

EXPERIMENTAL SECTION

Preparation of the ELPs. An inorganic salt-containing substrate, BSA-inorganic salt membrane was prepared as mentioned in our previous study.[1] In brief, 75 mg bovine serum albumin (BSA, purity >98%; Merck) was mixed with 15 mg six different inorganic salts ($Na_2HPO_4{\cdot}12H_2O$, $NaH_2PO_4{\cdot}2H_2O$, $K_2HPO_4{\cdot}3H_2O$, KH_2PO_4, NaCl, Na_2CO_3 and K_2CO_3) in 1mL deionized water, respectively. A droplet of the resulting solution, approximate 10μL, was added onto a silicon wafer or electrically conductive glass and dried out to form a membrane by put on a hot stage preheated at 55-60℃, for 1-2h under ambient conditions. The dried inorganic salt-containing substrate was then placed under appropriate RH (typically 50-60%) and room temperature (20-26℃) for the formation of ELPs on the surface of the substrate.

AFM observations and mechanical tests. An atomic force microscopy (AFM) instrument (Dimension Icon, Bruker) was employed to image ELPs formed on the surface of the inorganic salt-containing substrate. In tapping mode imaging, a probe cantilever with a normal spring constant of ~40 N/m and a resonant frequency of ~300 kHz (RTESP, Veeco) were used. In contact mode imaging, cantilevers with normal spring constants of 0.06-0.58 N/m (NP-S10 or SNL-10, Bruker) were applied. All images were captured with a scan rate of 1 Hz at room temperature. During the indentation tests, a contact-mode image of ELPs was first obtained with a slight force (to ensure the ELPs not being completely impaled), and then, a constant ramp rate of 1 Hz was chosen to carry out indentation tests on ELPs

XPS analysis. A X-ray photoelectron spectroscopy (XPS) instrument (ESCALAB 250Xi, Thermo Fisher Scientific) was used to analyze the surface elemental composition of ELPs under high vacuum condition (10^{-8}-10^{-7} Pa). Besides the survey spectra, high-resolution scans were conducted for individual elements including Na, K, P and O at pass energy of 30 eV. To obtain reliable results, the surface of all samples was etched by an argon ion beam at 2-3 keV for 15-30 s to generate a fresh surface for element analysis.

SEM imaging and EDS. A scanning electron microscope (SEM) (Quanta600 FEG, FEI) equipped with an energy dispersive spectrometer (EDS) (INCA Energy350, OXFORD) was used to image samples in low vacuum mode (90 Pa). For SEM imaging, an electrically conductive medium, electrically conductive glass, were utilized for preparing inorganic salt-containing substrate. During imaging, the accelerating voltage was set to 20 kV. For elemental analysis, the EDS was employed to obtain both the quantitative elemental composition and the qualitative elemental distribution map.

The phase transformation of phosphate salts in the water adlayer

To image the initial morphology of the substrate reliably, the substrate should be observed as quickly as possible (within minutes) by AFM when it is transferred from the hot stage (55-60℃) to room temperature (RH 50-60%). This guarantees that no excessive water vapor will adsorb onto the substrate surface and cause a significant change in morphology. After a period of time (ranging from minutes to several weeks), an increasing amount of water vapor condensed onto the substrate surface and new phases formed in the water adlayer (Figure S1A).

We traced the phosphate substrates with an AFM and found that they were unable to crystallize in the water adlayer but instead formed a large number of ELPs. The phase images showed that ELPs were generated during the nucleation stage and grew larger (to a maximum of more than 10 μm in lateral size, Figure S1B) during the later stages. During the whole growth process, all ELPs maintained a dark contrast in the images, which hints that the mechanical properties were most likely rather stable.

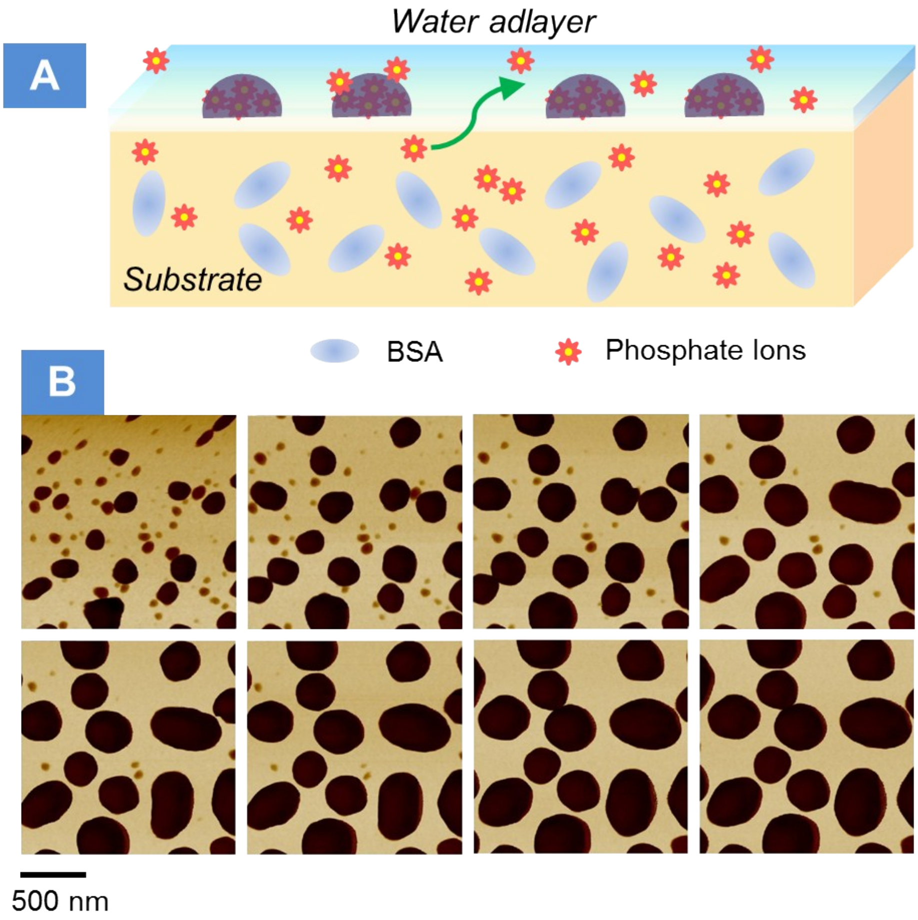

Figure S1. (A), AFM images (phase signal in tapping mode) and an optical image of a phosphate substrate that was transferred to room temperature (RH 50-60%) for a few hours and exhibits nucleation and growth of the ELPs.

The stability of ELPs

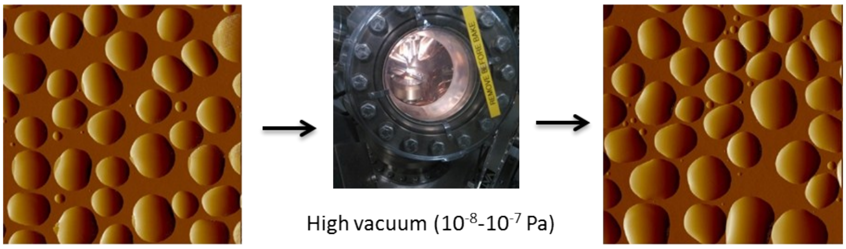

Figure S2. The tapping-mode AFM images of ELPs before (left) and after (right) processed with high vacuum (10^{-8}-10^{-7} Pa) for more than 48 h in an XPS chamber

The roles of BSA during the formation of the ELP

Two different substrates were especially designed to determine the role of BSA playing in the ELP formation. The first one is a salt-free substrate, containing BSA solely. After 48h incubation, no ELP was found on the substrate surface meaning that the formation of ELPs was mainly depend on phosphate salts and BSA on its own is unable to form a new surface phase, ELP (Figure S3A). The second substrate is a salt-containing BSA substrate coated with over 10nm gold layer that could completely block the diffusion of BSA molecules and only allow salt ions diffusing to the surface. The result AFM images showed that a few ELPs were formed, which confirm that BSA makes no contribution to the ELP formation, (Figure S3B)

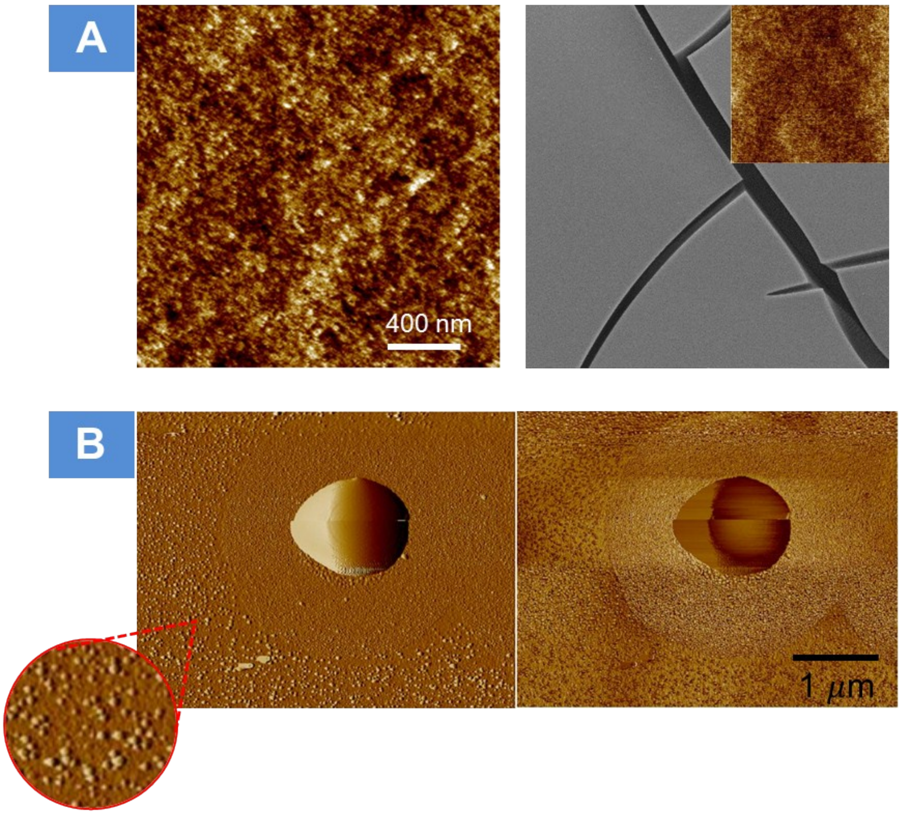

Figure S3. (A) The left is a substrate composed of solely BSA was prepared and imaged with tapping-mode AFM. (Right) After it was placed under an RH of 50-60% for more than 48 h, it was observed with tapping-mode AFM (inset) and SEM. (B) The tapping-mode AFM images of Au-coated phosphate containing substrate that was placed under an RH of 50-60% for7-10d. The left and the right are amplitude error and phase images.

EDS composition analysis of the ELP

In order to quantitatively analyzing the composition of ELPs, an EDS was used to test three areas, respectively, including a bigger ELP (1#), a smaller ELP (2#) and the blank surrounding area (3#). The results, shown in Figure S4 indicated that the content of elements P, O and Na increase with the increase in the ELP size. On the contrary, the content of element C decrease with the increase in the ELP size, and the highest content of element C is in the blank surrounding area. Therefore, the change of content of phosphates depends on the ELP size meaning that the major component of ELPs is phosphate salts.

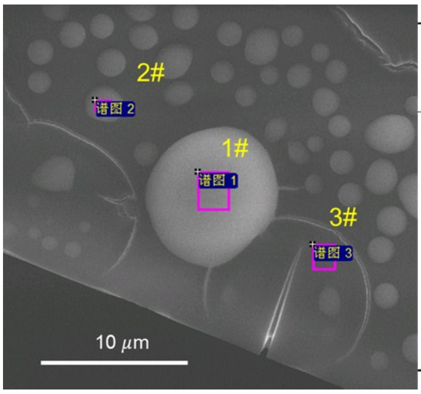

Spectrum	C	O	Na	P
1（$1^{\#}$）	15.84	55.91	15.13	13.12
2（$2^{\#}$）	37.2	48.86	7.07	6.87
3（$3^{\#}$）	51.94	39.16	4.28	4.62

Figure S4. For the ELPs of NaH_2PO_4, an EDS was used to quantitatively analyze the compositions of a bigger ELP (1#), a smaller ELP (2#) and the blank surrounding area (3#). The left is a SEM image of the ELP-covered substrate, and the right is the quantitative composition information of 1#, 2# and 3#.

XPS analysis of the ELP

XPS is a surface analysis technique that is usually able to measure the elemental composition of the top 10 nm of the material. To obtain reliable compositional information about the ELP, the substrate should be etched before analysis to remove adsorbates (as performed in “Experimental Section”). Moreover, the substrate must be covered with as many ELPs as possible to lower the impact of blank areas on the analysis of the ELP composition. Considering that XPS is usually unable to detect elements with an atomic number (Z) below 3 (Li) and that P and O are closely associated with phosphate groups, the water content can be estimated by the ratio of O/P (atom number ratio). This method is obviously not accurate under the influence of blank areas and uneven element distributions but is rather useful for approximate evaluation of the water content.

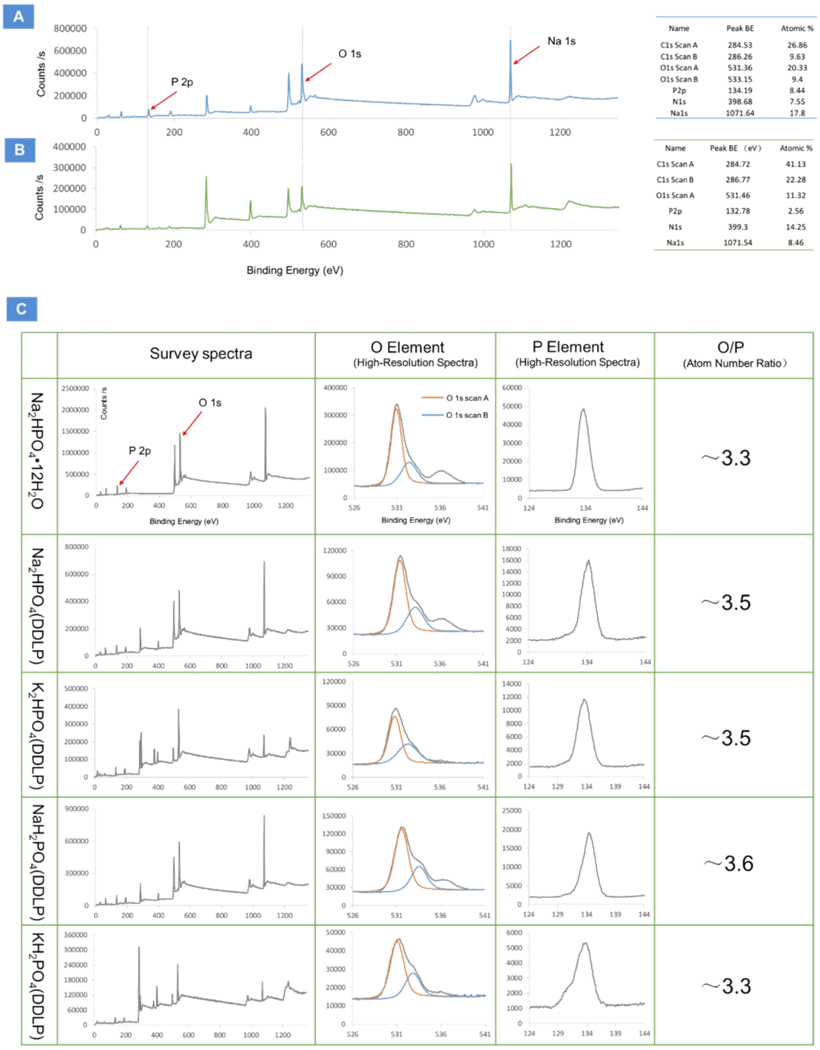

Name	Peak BE	Atomic %
C1s Scan A	284.53	26.86
C1s Scan B	286.26	9.63
O1s Scan A	531.36	20.33
O1s Scan B	533.15	9.4
P2p	134.19	8.44
N1s	398.68	7.55
Na1s	1071.64	17.8

Name	Peak BE （eV）	Atomic %
C1s Scan A	284.72	41.13
C1s Scan B	286.77	22.28
O1s Scan A	531.46	11.32
P2p	132.78	2.56
N1s	399.3	14.25
Na1s	1071.54	8.46

Figure S5. (A) The Na_2HPO_4-containing substrate covered with crowded ELPs. (B) The initial Na2HPO4-containing substrate without ELPs. (C) The content of the O and P elements in $Na_2HPO_4 \cdot 12H_2O$ (crystalline state) and four types of phosphate substrates (containing, respectively, Na_2HPO_4, K_2HPO_4, NaH_2PO_4 and KH_2PO_4) that are covered with crowded ELPs.

The core-shell construction of the ELP

We used a nanoindentor (Ti 950, Hysitron) to refine the core-shell model. The tip curvature radius of the nanoindentor probe is approximately 150 nm (Figure S6A), which is much larger than that (approximately 10-20 nm) of the AFM probe (Figure S6B). We used the large tip to contact the ELPs and examine what would happen. First, the tip was employed to contact a large (over 10 μm in lateral size) ELP (Figure S6C, indicated by the red arrow in the left image) and then was withdrawn. The resulting optical images indicated that the ELP became significantly smaller (Figure S6C, the second image). Second, the tip was controlled to repetitively contact the smaller ELP again, and it was determined that the smaller ELP did not decrease again but instead remained the same (Figure S6C, the third image). Third, the tip was employed a third time to contact a new bigger ELP, and the result indicated that the new ELP also became significantly smaller (Figure S6C, indicated by the yellow arrow in the right two images).

Obviously, this experiment strongly indicated the existence of a core-shell construction. During the first contact, the liquid-like shell of the ELP was easily attracted by the tip-induced capillary action and adhesion force and thus decreased. However, when the tip contacted the ELP the second time, the core was solid-like such that the tip was difficult to attract. That is why the ELP could maintain its size during the second contact. By that logic, when the third contact occurred on a new ELP, its liquid-like shell was attracted to the tip also and therefore decreased.

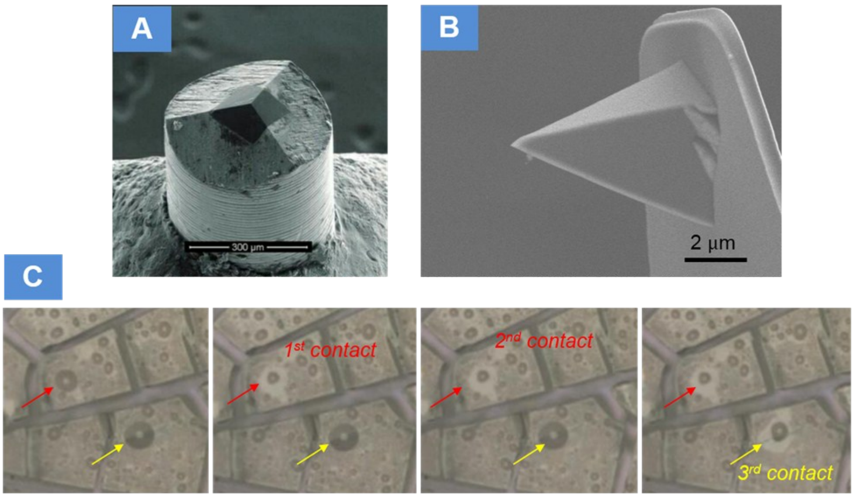

Figure S6. (A) and (B) are the probe SEM images of nanoindenter (Ti 950, Hysitron) and AFM, respectively. (C) A series of optical microscopic images (captured with integrated imaging system) to show the "core-shall" structure.

Reference

[1] Wang, Y.; Duan, Z.; Fan, D. Sci. Rep. 2013, 3505.